CHALMERS

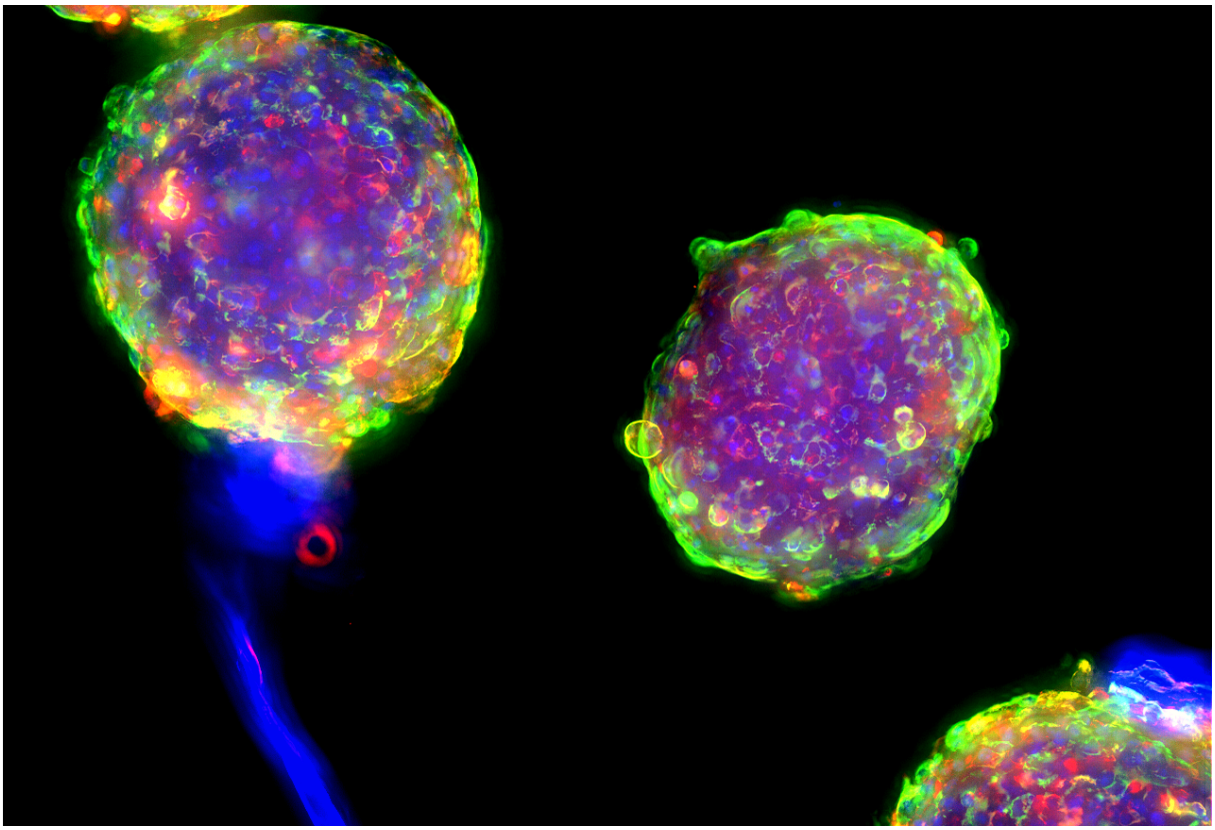

Development of a Hepatocyte Spheroid Culture Model for Drug Uptake, Metabolism and Transporter Studies

Master's of Science thesis in Biotechnology

Bhavik Chouhan

Department of Applied Physics, D*ivision of Biological Physics*
CHALMERS UNIVERSITY OF TECHNOLOGY
Gothenburg, Sweden 2015

Master's thesis 2015

Development of a Hepatocyte Spheroid Culture Model for Drug Uptake, Metabolism and Transporter Studies

Bhavik Chouhan

CHALMERS

Department of Applied Physics
Division of Biological Physics
CHALMERS UNIVERSITY OF TECHNOLOGY
Gothenburg, Sweden 2015

Development of a Hepatocyte Spheroid Culture Model for Drug Uptake, Metabolism and Transporter Studies
Bhavik Chouhan

© Bhavik Chouhan, 2015.

Supervisor: Tommy B. Andersson, AstraZeneca, Mölndal
Examiner: Julie Gold, Department of Applied Physics

Master's Thesis 2015
Department of Applied Physics
Division of Biological Physics
Chalmers University of Technology
SE-412 96 Gothenburg

Cover: High-Content Imagining of biomarkers CK18 (green) and CK19 (red) expressed in HepaRG spheroid culture after 10 day cultivation.

Abstract

The liver is a key organ in drug bioavailability including uptake, metabolism, and excretion as well as drug toxicity. Thus, a robust liver *in vitro* model that resembles *in vivo* micro environment with improved predictive capabilities is highly warranted. The focus in this thesis has been to develop and characterize a 3D liver spheroid model for the study of long-term drug uptake, metabolism, and transport. The bipotent progenitor cell line HepaRG has been used as it is known to express various liver specific markers and function in its differentiated state similar to primary human hepatocytes. Culturing these cells onto ultra-low attachment plates derived spheroid formation after 3 days independent of cellular concentration. Various staining techniques were used to investigate long-term sustainability of 2000 and 4000 cell spheroid culture. The gene expression analysis of the drug metabolizing cytochrome P450 (CYP) enzymes illustrated higher expression level in spheroid formation compared to 2D control while drug transporter, MRP2, hepatocyte markers Ki67, albumin, and CK19 all showed moderate to low expression. The HepaRG spheroid model showed promising results. The enzyme activity of CYP2C9, CYP2D6, and CYP3A4 was measurable throughout the whole cultivation period with a peak activity at day 7 while CYP1A2 showed no activity.

Acknowledgements

I would firstly like to thank my supervisor Tommy B. Andersson for presenting me with the opportunity of doing my master thesis at AstraZeneca and for all the guidance and useful input in this project.

Special thanks to

Annika Janefeldt and Kajsa Kanebratt, for their selfless and unending help throughout the whole project, and for all the very helpful discussion around the results.

Alan Sabirsh, for helping with the IF analysis of whole spheroid using the ImageXpress.

Anne-Christine Andréasson, for teaching and helping me with the paraffin embedding of spheroids.

Sepideh Hagvall, for walking me through and providing me the IF staining protocol.

Linda C. Andersson, for all the help and useful discussions regarding enzyme activity analysis of my spheroids.

A big thanks to Henrik Palmgren who has patiently answered my endless questions and helped me with most of the analytical methods used in this thesis.

My thanks also goes to all people in the CVMD DMPK group, AZ youths, friends outside of AstraZeneca and my family.

Table of Content

1. Introduction 9
   1.1. Background 9
   1.2. Aim 10
   1.3. Limitations 11
2. Theory 12
   2.1. General Liver Structure and Function 12
      2.1.1. Hepatocytes 12
      2.1.2. Non-Parenchymal Cells 12
   2.2. Liver *in vitro* Modeling 13
      2.2.1 Three Dimensional Liver Model 14
   2.3. Spheroid Culture Model 15
   2.4. HepaRG Cell Line 16
   2.5. Biomarkers for Studying Liver Models 16
      2.5.1. Cytokeratin 16
      2.5.2. Albumin 17
      2.5.3. Multidrug resistance-associated protein 2 17
      2.5.4. Ki67 protein 17
      2.5.5. Cytochrome P450 17
3. Material and Method 19
   3.1. Culturing HepaRG Cells 19
   3.2. Run I 19
      3.2.1. HepaRG Spheroid Culture 19
      3.2.2. HE and IF analysis 20
      3.2.3. RNA Isolation and Real-Time PCR analysis 21
   3.3. Run II 21
      3.3.1. HepaRG spheroid culture 21
      3.3.2. Immunoflourescent Staining of whole spheroids 22
      3.3.3. CYP1A2, CYP2C9, CYP2D6 and CYP3A4 enzyme activity 23
4. Results and Discussion 24
   4.1. Spheroid Development, Morphology and Handling 24
   4.2. HE and IF analyses of HepaRG spheroid sections 25
   4.3. Immunoflourescent staining of whole HepaRG spheroids 28
   4.5. Gene expression of HepaRG spheroid culture 29

4.4. CYP1A2, CYP2D6, CYP2C9 and CYP3A4 enzyme activity 31
5. Conclusion 34
6. Future Studies 34
Bibliography 35

1. Introduction

1.1. Background

The liver is one of the most complex organs in the body, handling numerous functions including protein synthesis, aiding in digestion, and detoxification of xenobiotic. This has made the understanding and studying of the liver a major challenge. It is known that organ and tissue formation *in vivo* occurs on the basis of coordination of cells in time and space through cell differentiation, polarity, morphology, mitosis, and apoptosis [2]. What is hoped to be achieved in the future is the ability to construct a fully functional *in vitro* liver model with *in vivo*-like resemblance that can be utilized for various purposes within different scientific fields.

The use of an appropriate *in vitro* model is, within the field of clinical pharmacology, highly important for the process of drug development as it gives initial affirmation of a drug to be systemically available and also interact with other drugs. A major problem encountered by several pharmaceutical companies is the inability to predict drug failure at an early stage in the drug development process. This subsequently leads to huge economical loss for the company, and drug or substance being withdrawn from the market [3, 4]. It has been estimated that a 10% improvement in prediction of drug failure could save $100 million, making the reason for finding a suitable *in vitro* model exceedingly relevant [5].

The setback lies in the current two dimensional (2D) *in vitro* models which fails to reconstruct a micro environment that resembles a living organism which prevents them to predict late stage drug failure [6]. This has as a result, during these past years, lead to 3D *in vitro* models garnering great attention. These models offer a more similar micro environment to *in vivo* with respect to cell shape, adhesion, behavior, topology, and morphology. Additionally they encompass the possibility of solving present challenges such as low cell viability, diverse phenotype expression and unnatural differentiation after isolation. An additional factor that contributes in producing a viable model is the choice of cell type. For optimal *in vitro* liver models, the use of primary human hepatocytes (PHH) is beyond compare however there are limitation in regards to drug deposition including, functional variability between donors, limited life span, and difficulties in maintaining differentiated phenotype after isolation [7]. In this project HepaRG cell line was used in a spheroid culture model. The HepaRG cell line is a bipotent progenitor cell line originated from a female patient suffering chronic hepatitis C infection and macro nodular cirrhosis [8]. It can differentiate towards two cell phenotypes namely: biliary epithelial cells and hepatocyte cells. In comparison to primary hepatocyte cells this cell line is more easily handled. HepaRG cells are utilized in this project due to its similarities with primary hepatocytes i.e. having the ability to express various types of liver specific enzymes and transporters in its differentiated state. Additionally, the gene expression level is known to follow a similar trend to primary hepatocytes.

The setback of existing 3D *in vitro* liver models is that they are technically challenging, labor intensive, and currently not suitable for high-through-put applications [9]. Most 3D systems additionally require an enormous amount of cells which depending on the cell type is not economically profitable. The use of spheroid culture models could solve some of the challenges mentioned above while at the same time maintaining an environment that

resembles *in vivo* morphology. As a 3D *in vitro* model it can also allow a more accurate translation of results to *in vivo* in comparison to conventional 2D models.

1.2. Aim

The aim of this project was to develop and characterize a spheroid *in vitro* model using HepaRG cell line that can be used for drug uptake, metabolism, and transport studies. This will be achieved by analyzing the initial applicability, morphology, physiology, and enzymatic activity of the model. The spheroids will be formed using non-adherent ultra low attachment plates (ULAP).

Initially, different spheroid sizes will be analyzed and observed for optimal analytical application. 3 different sizes were used with a cell density of 500, 2000 and 4000 cells. To understand the conformation and morphology of these spheroids they were observed during a cultivation period of 21 days. In this period of time a number of spheroids were sampled at day 3, 7, 10, 14 and 21 for sectioning and then analyzed using IF (immunoflourescent) and HE (Hematoxylin and Eosin) staining. The spheroids were also observed using a high-content screening microscope to better understand the polarization of certain liver specific markers including, MRP2, CYP3A4, CK18 and CK19.

Expressions of genes indentified in mature livers were studied at day 3, 7, 10, 14 and 21. The change in expression level over the cultivation period and between the different spheroids sizes were compared against a HepaRG 2D cultured control. The genes chosen in this thesis are: CYP1A2, CYP2C9, CYP3A4, MRP2, ALB, CK19 and Ki67.

To characterize the chronic functionality if the spheroids, phase I drug metabolizing enzyme activity was evaluated by pooling a number of spheroids at day 3, 7, 10, 14 and 21, and incubating them with a cocktail of drugs for 1h. The samples were collected and measured for the substances and their respective metabolites using LC/MS/MS (Triple-quadrupole). The cocktail substances, CYP enzyme targeted and metabolites formed are presented below in table 1.

Table 1. Drug substances used, CYP enzymes targeted and metabolites formed

Parent substance	CYP enzyme targeted	Metabolite
Phenacetin	CYP1A2	Paracetamol
Bufuralol	CYP2D6	1’-OH-Bufuralol
Diclofenac	CYP2C9	4’-OH-Diclofenac
Midazolam	CYP3A4	1’-OH-Midazolam

1.3. Limitations

Similar to most projects limitation where setup to accurately define the frame work within which I will progress. Since this thesis is a part of a larger project plan it has been restricted to focus on analyzing the initial applicability, morphology and functionality of the spheroid culture model using the HepaRG cell line. Simultaneously, suitable protocols for the various types of analytical methods used will be created and optimized. Secretion of albumin, urea and other compounds that defines a functional liver has not been performed as it has already been covered by previous studies [9, 10]. The drugs in this thesis have been selectively chosen as they reflect a large spectrum of drugs on the market that targets CYP enzymes abundantly found in the liver. This thesis has further more restricted the research to only include the phase I metabolic enzymes while excluding the phase II due to time limitations.

2. Theory

This chapter is aimed to give a theoretical understanding of the main concepts in this project while at the same time introducing specific terms, model used and substances investigated.

2.1. General Liver Structure and Function

The liver is one of the most versatile organs in the body as it deals with numerous functions including, metabolism of drugs, detoxification, emulsification of lipids, decomposition of red blood cells etc. The general gross anatomy of the liver is divided into 2 parts, the left and the right lobe by the falciform ligament. Oxygenated blood arrives from two sources namely, the portal vein and the hepatic artery. The portal vein supplies blood from the spleen and gastrointestinal tract which contributes to approximately 75% of the total blood supply while the remaining 25% is supplied by the hepatic artery from the heart [11, 12].

At a microscopic level it is observed that the liver consists of several types of cells which are broadly classified as either parenchymal (hepatocytes) or non-parenchymal cells (NPC) [12]. The NPCs are further divided into sinusoidal endothelial cells, Kupffer cells, stellate cells, biliary epithelial cells and natural killer cells. Other cell types do exist but in much smaller quantity. The broad variety of cell types and their different functional properties makes the liver a highly complex organ.

2.1.1. Hepatocytes

Hepatocytes are the most abundant cell type found in the main parenchymal tissue and it makes up approximately 80% of the total tissue volume and 60% of the total cell population of the liver. They are polarized in a way that they comprise 3 membrane domains: sinusoidal, lateral and canalicular. The sinusoidal domain functions as a carrier for blood to flow from the portal vein and hepatic artery to the central vein. It is lined with endothelial cells, Kupffer cells, and fat cells. The canalicular domain transports bile produced by the hepatocytes to the bile duct while the lateral surface creates tight junctions separating the canalicular domain from the basolateral surface [12].

Hepatocytes are the most active cell type in the liver performing numerous complex and important functions including: detoxification, synthesis and metabolism of various compounds and substances which is why they are extensively used in many experimental methods [7, 12]. The aim of using hepatocyte culture is to construct a model that is able to function and respond in a physiological manner similar to *in vivo*. In addition, it is also sought to achieve long-term cultivation of hepatocytes without adverse or reduced phenotypic expression levels. It is hence important to be able to define hepatocytes. This can be done by including both qualitative study of the presence/absence of hepatocyte markers and enzymatic activity evaluation [12].

2.1.2. Non-Parenchymal Cells

Although the majority of the liver consists of hepatocytes, NPCs also play an important role as they aid in the growth, metabolism and transport function of hepatocytes [12]. There are, as mentioned previously, 5 major non-parenchymal cell types: liver sinusoidal endothelial cell (LSEC), Kupffer cells, stellate cells, biliary epithelial cells, and natural killer cells. LSECs are characterized by fenestration and the lack of basement membrane. They performs the basic

functions such as delivery of oxygen, nutrients and other maintenance factors to the underlying tissue while removing waste and breakdown factors from it [12]. In addition LSEC participates in inflammatory reaction mechanisms including detection of pathogen associated molecular patterns, secretion of cytokines and chemokines, and involvement in adhesion and diapedesis of leukocytes [7, 12]. Kupffer cells are specific macrophages located inside the sinusoidal space and are utilized by the tissue as a defense mechanism to destroy damaging foreign material. The space between hepatocytes and LSEC is known as 'Space of Disse' which is where the stellate cells are situated. They are involved mainly in liver fibrosis. Cholangiocytes or biliary epithelial cells (BEC) makes up the biliary tract in the liver tissue and actively participate in the secretion of bile via the canalicular network as well as mucin secretion and reparative function in disease conditions.

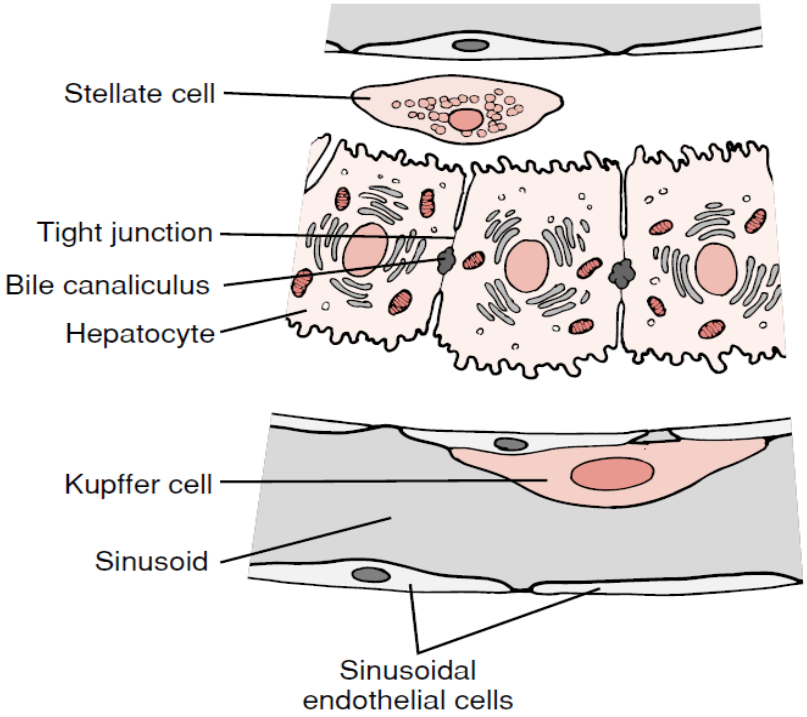

Figure 1. A schematic picture of the various cell types found in the liver tissue [1].

The ability of these different cells types to entwine and co-operatively interact with each other demonstrates the complexity of the liver's structure and functionality. Hence, studying and developing an *in vitro* model that is able to as closely as possible mimic the *in vivo* environment is extremely difficult and requires the ability to overcome a multitude of obstacles.

2.2. Liver *in vitro* Models

Developing an *in vitro* model that is able to encompass the functionality and mimic the microenvironment of *in vivo* system is highly important within several scientific fields and is perused by scientists both in academics and industries. Pharmaceutical companies use these models in the process of drug development to attain initial data and understanding of a drug allowing them to affirm if it should pass to *in vivo* studies or not. One of the major problems pharmaceutical industries face is drug induced liver injuries (DILI) as a result of late stage

drug failure. Animal studies and *in vitro* models combined have limited predictive capabilities. Previous surveys have shown that 38-51% of the DILI is not detected at a preclinical stage [13]. The inability of these models to detect drug failure at an early stage leads to huge economical loss for the company, and drug or substance being withdrawn from the market. Developing and improving the prediction capability of *in vitro* model allows the drug development process to be more cost-effective and it would also reduce the need for animal studies considerably [2, 14, 15]. In an article written by Sasseville *et.al.* (2004), it was estimated that even a 10% improvement in prediction capability of drug failure could save $100 million, making the reason for finding a suitable *in vitro* model exceedingly relevant [5].

An optimal liver *in vitro* model should, as mentioned in an article review written by Arto *et.al.* (2014), generate a natural environment where cells can express an *in vivo*-like phenotype, be able to promote co-culture of multiple cell types, enable high-throughput screening and be utilized for PK/PD and toxicology studies giving relevant results [16]. To construct such a model one needs to consider the current 2D models and their drawbacks. These models have allowed us to understand and determine several biochemical reactions, topological features and other initial cell related systems. They are suitable for various experimental procedures including determining mitotic potential of cells, change in cell functional activity when put under impact of specific factors and biochemical characterization of cells [17]. The most extensively used 2D *in vitro* models are cells in either suspension or monolayer were the cell type used are either primary cells or a cell lineage. When cultured in suspension cells have minimum to no cell-cell interaction which results in declining viability and functionality within a couple of hours. Cells grown in monolayer, on a flat-bottom plastic or film coated layer, interact more with other nearby cells allowing the phenotypic expression to survive for a slightly longer period of time. However the plastic surface represents an unnatural environment for the cells which could allow for deviant phenotypic expression of certain genes as well as abnormal cell morphology, proliferation and adhesion [18]. While both of these models are simple, cost-efficient and high-throughput it is noticeable that they lack the ability to create a suitable environment for cells to survive and function for a longer period of time. Hence, in recent years three dimensional (3D) models have garnered great attention as the construction of these models are able to mimic and closely replicate *in vivo*-like systems.

2.2.1 Three Dimensional Liver Model

Escalating development, in current years, within the field of biomaterial and tissue engineering has simultaneously created and improved various forms of 3D *in vitro* models that can be utilized to better comprehend cellular systems. The basis of these models is to mainly maximize cell-cell interaction [15, 19, 20]. This enables cells to create a communicative network which promotes a behavior similarly found in the natural tissue. The 3D structure enhances different cellular mechanisms such as: proliferation, differentiation, morphology, migration, signaling, etc. [15, 19-21]. It has also been illustrated that the close interaction and communication between cells also extends their viability [14].

3D *in vitro* models are mainly divided into two categories depending on the use of scaffold or not. The majority of models are scaffold based which allows for a more complex construct that closely resembles *in vivo* micro environment to be developed. The scaffold material can

either be some form of hydrogel-based matrices or a more solid material. The evolution of tissue engineering and biomaterials have allowed a wide range of techniques and materials to be developed with diverse physical and biological properties that takes into account different cell types and/or cell mechanisms [12, 14, 22]. One of these techniques includes the ability to decellularize a whole organ from any species leaving behind the extracellular matrix which can be used as a scaffold. Decellularization allows most ECM components to be preserved, which are believed to play an important role in various cellular mechanisms including: migration, proliferation, differentiation, etc. [23]. Another benefit of this technique is that it avoids the problem of creating a vascular network that is used for the purpose of supplying oxygen and other required nutrients to the cell. After the organ has been decellularized it can be repopulated with human cells alternately to its other cell type allowing it to closely resemble equivalent human organ. 3D bioprinting is another scaffold based techniques which applies the use of 3D printing technology to position cells, embedded in some type of hydrogel, with great accuracy and precision [24]. However most of these models are expensive due to complexity of the equipments used and the extensive amount of cells needed. Additionally, those models are difficult to replicate and are currently not suitable for high throughput applications. Spheroid culture on the other hand which is a 3D scaffold-free model requires fewer cells making it an inexpensive model, is much less complex in comparison to the scaffold based models and it can be used for high throughput applications [9].

2.3. Spheroid Culture Model

One of the first liver spheroid models developed and studied was by Landry *et.al.* in 1985. They isolated and seeded rat liver cells onto a non-adherent plastic substratum which directed the cells into forming aggregates within the span of 1-2 days [25]. The use of spheroids has since greatly improved while simultaneously maintaining the simplicity and increasing its applicability. The general concept of the spheroid model is to seed single cells into a well or a vessel and through gravity allowing the cells to sediment to the bottom were they aggregate to form a spheroid as described in figure 2 bellow. Different types of spheroid models are currently at use which includes Insphero's hanging drop technique, plates with non-adherent surface or rotating vessels [16, 21]. Using this technique, the cells are known to improve cellular communication which allows for increased viability of cells as well as prolonged phenotypic expression in comparison to 2D *in vitro* models. Since the environment created resembles *in vivo*, cells are able to maintain their cellular functionality much longer [9, 10, 18, 21, 26].

As mentioned previously, most 3D models require some form of a scaffold to uphold the construct and for spatial control. Spheroid culture model however requires no scaffold as the cells independently rearranges and constructs the structure. While this makes the model simple and more cost-efficient, it does deprive the ability to form complex structures and to attain an organized a co-culture.

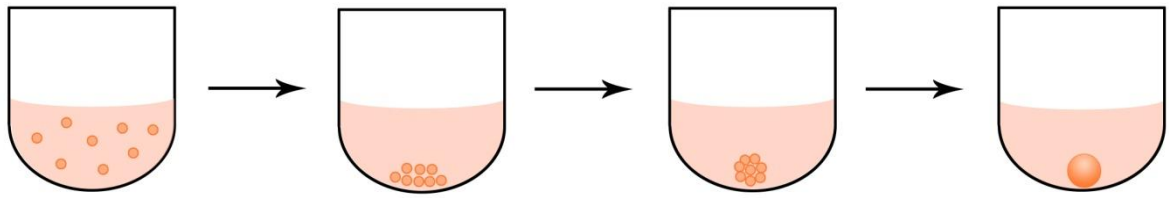

Figure 2. General concept of spheroid development.

2.4. HepaRG Cell Line

HepaRG is bipotent progenitor cell line that originates from a female patient suffering chronic hepatitis C infection and macro nobular cirrhosis. It has two distinctive phenotypes which allow it to differentiate into either hepatocytes or BECs [8, 27, 28]. The reason for its increased used in recent times has to do with its ability to express various types of CYP enzymes (CYP1A4, 2C9, 2D6 and 3A4), phase II to enzymes (glucuronosyltransferase, N-acetyltransferase and sulfotransferase), nuclear receptors (PXR, PPARα), transporters (MRP2 and MDR1) among other liver specific proteins in its differentiated state. The use of the HepaRG cell line in constructing 3D models has shown to extend the gene expression levels for a longer period of time. The expression level has additionally shown to resemble that of PHH giving a closer translation of *in vitro* results to *in vivo* culture [28]. The cells are also able to sustain its function longer, making it applicable for chronic studies of diseases and drugs. These factors make the use of the HepaRG cell line in developing an *in vitro* model highly suitable [27].

2.5. Biomarkers for Studying Liver Models

A vital step in developing a liver *in vitro* model is to observe the presence/absence and expression of certain markers that are abundantly found in the liver and in cells generally. The markers in this thesis have been chosen to primarily give information on the two different cell types expressed by the HepaRG cell line and to observe markers that play important role in the function of those cells. The markers that have been included are cytokeratin 18 (CK18), cytokeratin 19 (CK19), albumin (ALB), Multidrug resistance-associated protein 2 (MRP2), Ki67 and CYP enzymes (CYP1A2, CYP2C9, CYP2D6 and CYP3A4).

2.5.1. Cytokeratin

Cytokeratins are proteins that contain keratin in their intermediate filament and are usually found in the epithelial tissue. They are divided into two main types based on their polarity; there is the basic to neutral type II cytokeratins and the acidic type I cytokeratins. Type II ranges from CK1-8 while type I includes CK9-20 [29, 30]. Cytokeratins are expressed in various concentrations depending on the organ or tissue observed and can therefore be used as markers for identification. Going back to the two Cytokeratins used in this thesis, CK18 is highly expressed in hepatocytes whereas CK19 is more abundantly found in BECs. However whether or not the expression of CK19 is restricted to biliary cells is still to be studied [8].

2.5.2. Albumin

The water-soluble albumin family is a globular protein and it is found mainly in the blood plasma were its purpose is to regulate osmotic pressure of the blood. The liver and more specifically hepatocytes perform several significant functions in the body of which one is production of proteins that are essential to blood clot formation. Albumin is one of those proteins produced. The state of the liver can to some extent be predicted measuring the concentration of albumin. Low concentration of this protein indicates some form of dysfunction in the liver. Hence it is often used to attain preliminary understanding of the state and function of hepatocytes [31, 32].

2.5.3. Multidrug resistance-associated protein 2

MRP is a transmembrane transporter that belongs to the ATP-binding cassette (ABC) superfamily [33]. It is mostly expressed in the canalicular membrane of hepatocytes. There it serves as a defense mechanism in the cells to eliminate eminent threats such as disease-causing microorganism, drugs, and chemicals among other things [34]. Studies have suggested that it is involved in cancer drug resistance by transporting the drug against the concentration gradient [35, 36]. In addition, it can transport a wide range of organic and anionic conjugates [33-35].

2.5.4. Ki67 protein

The Ki67 protein expression is associated with cell proliferation and is present during the active part of the cell cycle (G_1, S, G_2 and mitosis) whilst being absent during the resting phase (G_0) [37]. This makes it a suitable marker for various type of analysis involving the growth of cell population [37].

2.5.5. Cytochrome P450

One important liver function is the ability to metabolize xenobiotics. Through evolution the body has developed a mechanism where it is able to excrete various forms of xenobiotic drugs [38, 39]. Most xenobiotic drugs have to go through at least one of two enzymatic systems, phase I and/or phase II . During phase I reaction the parent compound is converted into a more hydrophilic compound by adding or removing a functional group (-OH, -SH, -NH2, COOH, etc.) [38, 39]. Phase I enzymes mainly includes Cytochrome P450 which constitutes as the largest enzyme family abundantly found in the liver, gastrointestinal tract, lung and kidney. These enzymes are utilized for drug and other lipophilic xenobiotic metabolism. The phase II system involves conjugating or synthetic enzymes. Examples of these enzymes are sulfotransferases (SULT), UDP-glucuronosyltransferases (UGT), glutathione-S-transferases (GST) and N-acetyltransferases (NAT). This thesis will however only focus on the phase I enzymatic system including 4 main CYPs namely: CYP1A2, CYP2C9, CYP2D6 and CYP3A4.

The CYP1A2 enzyme is involved in the metabolism of xenobiotics through hydroxylation and other oxidative transformation of aromatic amines and heterocyclic compounds [40]. As it is highly expressed in the liver it possesses a significantly important role in metabolism of pharmacological drugs. These include analgesics, antipyretics, antidepressants, anti-inflammatory, cardio vascular drugs, etc [40]. CYP2C9 the major enzyme expressed in the CYP2C family is involved in the metabolism of anticoagulants, anticonvulsants, anti-diabetics

and anti-inflammatory drugs [40, 41]. Diclofenac and tolbutamide are common substrates used when phenotyping CYP2C9 [40]. The CYP2D6 is the only protein in the CYP2D family. In contrast to its low expression in the liver it metabolizes almost a fourth of all clinically used drugs from several therapeutic classes [42]. These include antiarrhythmic, antipsychotic and β-blockers among others [40]. CYP3A4 is characterized by its large and flexible active site allowing it to metabolize larger lipophilic compounds. These larger substrates are often immunosuppressants, anti-cancer drugs, several endogenous drugs etc. [40].

3. Material and Methods

The experimental procedure was divided into two main runs which are described in more details in this section of the report.

3.1. Culturing HepaRG Cells

Cryopreserved differentiated HepaRG cells (Biopredic International) were thawed and seeded according to the manufacturer's instructions with slight modifications made to suit the experiment. The medium used for thawing and seeding consisted of William's E Medium (without phenol red or L-glutamine) supplemented with GlutaMAX™-I (Invitrogen Life Technologies) and additive ADD671 (Biopredic International). On day 3, 50% of the medium was replaced with William's E medium, GlutaMAX™-I and additive for maintenance/metabolism, ADD621 (Biopredic International) which is referred to as culture medium in this thesis. The ADD621 contains 2% Dimetylsulfoxid (DMSO). The culture medium was there after exchanged every 2-3 days during the cultivation period of 21 days. For CYP activity experiments the medium used was William's E, GlutaMAX™-I supplemented with serum-free induction additive, ADD651 (Biopredic International). The cells where maintained in a sterile environment at 37^{o}C, 95% air and 5% CO_2. Details of each individual procedure are explained further under each subsection.

3.2. Run I

The first run focused mainly on attaining a suitable spheroid size for various types of analysis. The sizes chosen were 500, 2000 and 4000 cells per spheroid. These sizes were sampled after 3, 7, 10, 14 and 21 days for gene expression, HE and IF analysis.

3.2.1. HepaRG Spheroid Culture

HepaRG cells were seeded onto 5 ultra-low attachment plates, one for each sample day, with the 3 different cellular concentrations as described below in the cell seeding layout.

Cell seeding layout

1	2	3	4	5	6	7	8	9	10	11	12
13	14	15	16	17	18	19	20	21	22	23	24
25	26	27	28	29	30	31	32	33	34	35	36
37	38	39	40	41	42	43	44	45	46	47	48
49	50	51	52	53	54	55	56	57	58	59	60
61	62	63	64	65	66	67	68	69	70	71	72
73	74	75	76	77	78	79	80	81	82	83	84
85	86	87	88	89	90	91	92	93	94	95	96

500 cell spheroids

2000 cell spheroids

4000 cell spheroids

The spheroid formation, morphology and maintenance was followed using a Nikon Eclipse TE2000-U microscope coupled with ACT-1 Nikon software during the whole cultivation period of 21 days.

3.2.2. HE and IF analysis

HepaRG spheroids of each size and from each sample day were collected into 1,5mL eppendorf tubes. Every sample contained 4-6 spheroids. The spheroids were first washed 2x with PBS (-$CaCl_2$/-$MgCl_2$) where after they were incubated with 150µL 4% paraformaldehyde (PFA) overnight at 4°C. The next day they were washed again 2x with PBS. Spheroids were then encapsulated using HistoGel™ Specimen process gel (Richard-Allan Scientific) to ensure proper paraffin embedding. After the spheroids had been encapsulated, each sample went through dehydration and paraffin infiltration steps. The samples were then embedded in paraffin blocks and submitted to Histo-Center AB (Göteborg, Sweden) for sectioning and HE staining process.

For IF analysis, sections of the paraffin embedded samples attained from Histo-Center were initially deparaffinized and rehydrated. Primary (purchased from abcam) and secondary antibodies presented bellow in table 2 were used for double staining of the spheroid sections.

Table 2. Details of primary and secondary antibodies used for IF staining spheroid sections.

1° Antibody	Dilution	Anti-	Raised in	2° Antibody	Dilution	Anti-	Raised in
CYP3A4	1/50	Human	Rabbit polyclonal	Alexa Fluor® 555 dye	1/500	Rabbit	Goat
MRP2	1/200	Human	Mouse monoclonal	Alexa Fluor® 488 dye	1/400	Mouse	Goat
CK18	1/50	Human	Mouse monoclonal	Alexa Fluor® 488 dye	1/500	Mouse	Goat
CK19	1/100	Human	Rabbit monoclonal	Alexa Fluor® 555 dye	1/400	Rabbit	Goat

After rehydration, sections were permeabilized by incubating them in 0.25% Triton-X, 0.01% Tween-20 in PBS. Before adding the primary antibodies the section were incubated in serum blocking agent (specific to the secondary antibody) to prevent nonspecific binding of the primary antibody. The serum blocking consisted of 1% bovine serum albumin (BSA), 2% goat serum (secondary antibody specific), 22.52mg/mL glycine, 0.075% Triton-X and 0.01% Tween-20 in PBS. The sections were then incubated with a mixture of the two primary antibodies of interest in serum blocking solution (without glycine) for 1h where after the sections were washed 3x in 0.1% Tween-20 in PBS. The secondary antibody mixture was then added and sections were incubated for approximately 30-60 min. They were then washed 3x15 min with PBS, counterstained with Hoechst (1:2000 dilution) for 1 min and then rinsed with PBS. A drop of mounting medium was added to the slide and sealed with a coverslip. All the samples were stored in darkness at 4°C. IF and HE samples were observed using Zeiss Axioskop flourescent microscope coupled with Infinite Analyzer software.

3.2.3. RNA Isolation and Real-Time PCR analysis

RNA isolation was performed by pooling together 9 spheroids of each spheroid size and sample day. On day 7 a single spheroid of each size was additionally isolated to test the possibility of gathering gene expression data from such a small sample. Isolation and extraction of RNA was done using RNeasy Micro Kit (Qiagen) following the manufacturers protocol with some minor modifications. Purity of RNA was measured using an Agilent RNA 6000 Nano Kit on an Agilent 2100 Bioanalyser. The instrument measures RNA concentration of each sample as well as the RNA integrity number (RIN). The RIN value is calculated by measuring the ratio of 28S:18S ribosomal RNA. A RIN value above 8 is considered pure enough to proceed. After analyzing the purity of each RNA sample they were converted into cDNA using Superscript III First-Strand Synthesis System (Invitrogen, Life Technologies) according to the manufacturer's instructions. Primers used for qPCR were CYP1A2, CYP2C9, CYP3A4, albumin (ALB), MRP2, cytokeratin 19 (CK19) and Antigen KI67 (Ki67), all acquired from Life Technologies. The reactions were performed on a QuantStudio™ 7 Flex Real-Time PCR System (Life Technologies). Through the use of Livak or ΔΔCt method, Ct values obtained from various genes expressed were compared to glyceraldehyde 3-phosphate dehydrogenase (GAPDH) which is a known endogenous control. A known HepaRG 2D cultured sample was used to further calculate the fold-change by normalizing the mRNA level of the spheroid cultured samples to the known 2D cultured sample.

3.3. Run II

From the first run it was concluded that handling and analyzing the 500 cell spheroid size was too demanding, it was hence excluded from further experiments in this thesis. The second run focused mainly on determining the CYP activity of the 2000 and 4000 cell spheroids using high-content imagining of whole spheroids and gene expression analysis. Gene expression analysis was further experimented on to obtain a more refined protocol and to achieve better results. Details on these experiments are further presented below.

3.3.1. HepaRG spheroid culture

HepaRG cells were seeded into 11 ULAP out of which 5 were used for CYP activity testing and gene expression analysis, 3 plates for fluorescent staining and high-content imagining and the remaining were extra plates. The cell seeding layouts differed slightly depending on the type of analysis and are presented below.

Gene Expression and CYP activity

1	2	3	4	5	6	7	8	9	10	11	12
13	14	15	16	17	18	19	20	21	22	23	24
25	26	27	28	29	30	31	32	33	34	35	36
37	38	39	40	41	42	43	44	45	46	47	48
49	50	51	52	53	54	55	56	57	58	59	60
61	62	63	64	65	66	67	68	69	70	71	72
73	74	75	76	77	78	79	80	81	82	83	84
85	86	87	88	89	90	91	92	93	94	95	96

2000 cell spheroids

4000 cell spheroids

Fluorescent staining

1	2	3	4	5	6	7	8	9	10	11	12
13	14	15	16	17	18	19	20	21	22	23	24
25	26	27	28	29	30	31	32	33	34	35	36
37	38	39	40	41	42	43	44	45	46	47	48
49	50	51	52	53	54	55	56	57	58	59	60
61	62	63	64	65	66	67	68	69	70	71	72
73	74	75	76	77	78	79	80	81	82	83	84
85	86	87	88	89	90	91	92	93	94	95	96

Day X 2000 cell spheroids

Day Y 2000 cell spheroids

Day X 4000 cell spheroids

Day Y 4000 cell spheroids

3.3.2. Immunoflourescent Staining of whole spheroids

HepaRG spheroids cultivated until day 3, 7, 10, 14 and 21 were collected into 1,5mL eppendorf tubes, 5 per size and type of staining. The spheroids were first washed with PBS 2x and then fixated with 4% PFA for 20-25min at room temperature. They were then washed 3x with PBS and stored at 4°C for staining and imagining. The spheroids were stained as described previously in the IF analysis section leaving out the deparaffinization and rehydration step. Below is a table showing details on dilution factors used for primary and secondary antibodies.

Table 3. Details of primary and secondary antibodies used for IF staining whole spheroids.

1° Antibody	Dilution	Anti-	Raised in	2° Antibody	Dilution	Anti-	Raised in
CYP3A4	1/60	Human	Rabbit polyclonal	Alexa Fluor® 555 dye	1/500	Rabbit	Goat
MRP2	1/200	Human	Mouse monoclonal	Alexa Fluor® 488 dye	1/400	Mouse	Goat
CK18	1/40	Human	Mouse monoclonal	Alexa Fluor® 488 dye	1/500	Mouse	Goat
CK19	1/80	Human	Rabbit monoclonal	Alexa Fluor® 555 dye	1/400	Rabbit	Goat

For Imaging of whole spheroids, samples were transferred onto a Collagen I Clear well 96-well Black/Clear Plate (354649, Corning® BioCoat™). To avoid spheroids being adhered to the pipette tip, they were first dipped into a solution containing 0,1% BSA in PBS. The stained spheroids were observed using ImageXpress Micro XLS Widefield High-Content Analysis System (Molecular Devices) with MetaXpress software.

3.3.3. CYP1A2, CYP2C9, CYP2D6 and CYP3A4 enzyme activity

One day prior to the experiment, 80µL of HepaRG culture medium was switched to 80µL HepaRG serum-free induction medium in the plate used for CYP activity analysis. On the day of the experiment, approximately 30 spheroids of each size were pooled together into two separate wells of a cell culture, 96-well, flat-bottom plate (Corning® Costar®). Excess medium was removed from each well leaving 50µL of HepaRG® serum-free induction medium. A 50µL volume of twice as concentrated cocktail was added to each spheroid pool giving a final concentration of each substance as described below in table 4.

Table 4. Concentration of cocktail before and after adding it to the spheroid pool

	Cocktail Concentration [µM]	Final Concentration [µM]
Phenacetin (CYP1A2)	52	26
Midazolam (CYP3A4)	6	3
Bufuralol (CYP2D6)	40	20
Diclofenac (CYPC9)	18	9

The samples were incubated for 1h during which the plate was removed from the incubator and slightly tapped every 15min to keep spheroids from aggregating. Images of pooled spheroids before and after incubation were taken in order to confirm if any aggregation occurred. The sample activity was terminated after 1h by transferring 50µL each sample to a plate containing 100µL of 300nM 39:an (5,5-dimethyl-1,3-diphenyl-2-iminobarbituric acid, internal standard) and 0,8% formic acid in acetonitrile. A standard curve was prepared on the same plate to measure the amount of metabolites formed after 1h of incubation. The metabolites investigated were paracetamol, 1'-OH-midazolam, 4'-OH-bufuralol and 4'-OH-diclofenac starting from a concentration of 9µM and diluted with a factor of 3.

After adding the standard curve to the plate it was centrifuged for 20min at 4000x*g* and 4^{o}C. The samples were then diluted 1:1 with dH_2O on a new plate which was centrifuged for 5min at 4000x*g* and 4^{o}C. All CYP activity analysis was performed using LC/MS/MS (Triple quadrupole). The column used for this experiment was an Atlantis C18 column from Waters with a non-polar stationary phase and 3µm particle size. The dimensions of the column was 30 mm (length) x 2,1 mm (diameter). Two mobile phases were used. Mobile phase A consisted of 2% acetonitrile and 0,2% formic acid in dH_20. Mobile phase B of 0,2% formic acid in acetonitrile.

RNA isolation and extraction was performed by collecting the spheroids used for CYP activity measurement (~30 spheroids). Similar protocol and genes as described under the previous q-PCR section in run I was used.

4. Results and Discussion

Results obtained from various analyses are explained, presented and discussed in this chapter in the form of figures and graphs.

4.1. Spheroid Development, Morphology and Handling

The plated HepaRG cells were during both runs followed for the whole cultivation period of 21 days. Figure 3 below, illustrates the aggregation of cells to form a spheroid structure already after 3 days independent of cellular concentration. The structures were observed to be more definite at day 4 from which it is possible to distinguish the 3 seeding densities of 500, 2000 and 4000 cells. The approximate diameter of each size was measured during the first run to 180, 250 and 350 µm for 500, 2000 and 4000 cells respectively. No significant change in spheroid sizes was observed during the whole cultivation period.

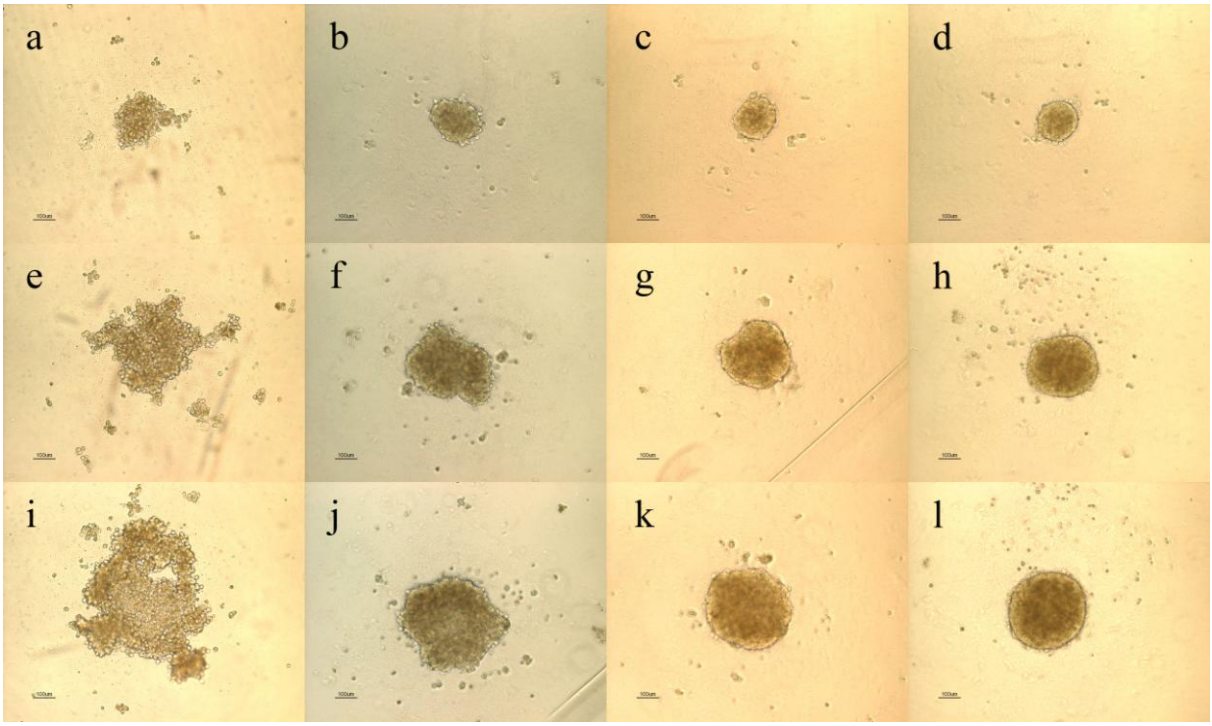

Figure 3. Development of HepaRG spheroid over a 4 day period. a-d) 500 cell spheroids, e-h) 2000 cell spheroids and i-l) 4000 cell spheroids.

The spheroid structure was still visible even after 21 days however the outer layer of the two larger spheroid sizes were observed to somehow deteriorate and excrete some form of debris as illustrated in figure 4. This destabilization of structure towards the end of the cultivation period could possibly be an initial indicator of the declining CYP activity presented and discussed later on in this chapter.

Difficulties in handling spheroids proved to vary between sizes both when changing medium and when utilized for analytical experiments. Overall, it was easier to handle the two larger sizes as they were visually observable. The smaller size on the other hand required an enormous amount of concentration and patience which took the experiment almost twice as much time as the two larger spheroids. Additionally, the small size of 500 cells made it difficult to be certain if the numbers of counted spheroids were present for various

analytical methods. This was especially true when encapsulating the spheroids using HistoGel before paraffin embedding. As a result, it was after the first run decided that the 500 cell spheroids size would not be used for later analysis.

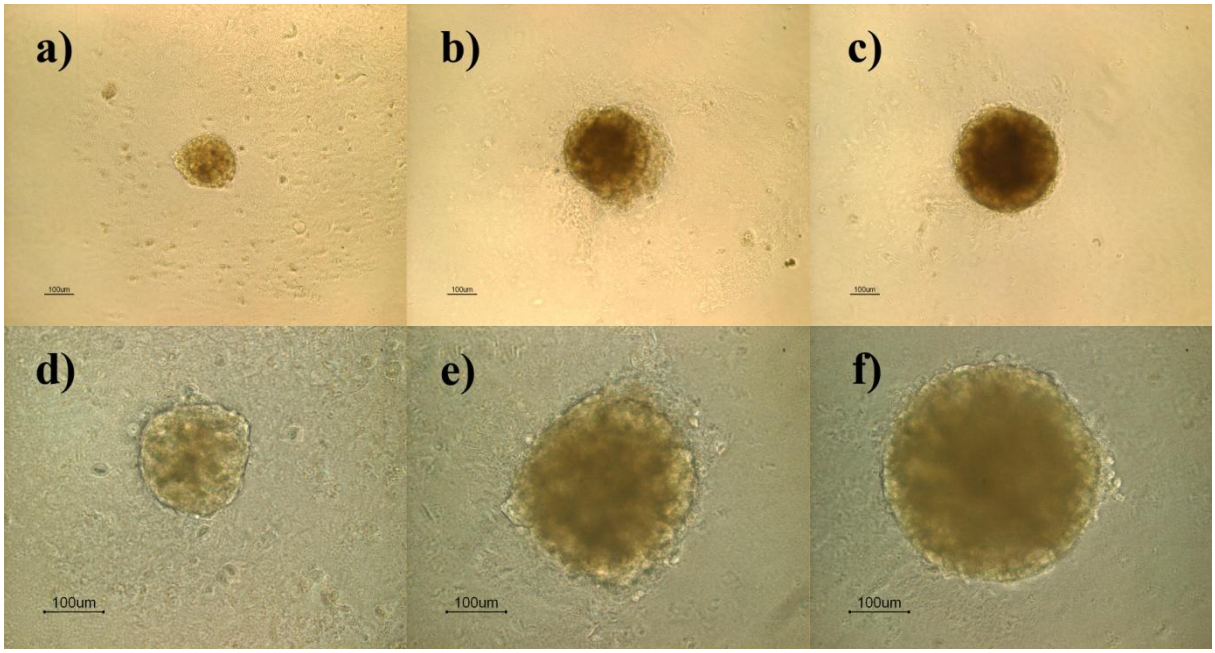

Figure 4. Morphology of the 3 spheroid sizes at day 21. a-c) 10x magnification, d-f) 20x magnification.

4.2. HE and IF analyses of HepaRG Spheroid Sections

It proved to be difficult to find and section samples containing only 4-6 spheroids. Histocenter therefore decided to section the same spheroid several times. As a result the sections stained with HE seems to be similar in size, see figure 5, however it should be noted that this is not the case. The section stained with primary antibodies on the other hand seems to concur with the actual sizes. It was uncertain if any 500 cell spheroids were present in the paraffin embedded samples and this was proved to be true when sectioned. It is speculated that the few number of cells used to paraffin embed in combination with its small size might have result in loss of sample. This contributes to the impracticality of the smaller spheroid size adding to the reason for not continuing with it even though the structure is seen to be kept stable for the whole cultivation period.

The HE staining is an acid-base combination staining technique. Eosin which has a basic structure stains the acidic cytoplasmic components while hematoxyline with its acidic structure stains the basic components in the nucleus. The obtained section of spheroids stained with HE shows the presence of cells close to the center of the spheroid. One of the problems encountered when using this type of models is the formation of necrotic core which is a result of poor diffusion of oxygen, nutrients and other substances that are important to sustain cellular function. The formation of a necrotic core in HE staining is often visualized as a lighter area at the center due to absence of cells [43]. Through observing the HE staining of 2000 and 4000 cell spheroids at day 8 and day 14 (figure 5 and 6) it is clearly illustrated that no necrotic core has been formed. However it should be taken into consideration that the size of both 2000 and 4000 cell spheroid sections is almost the same when looking at figure 5 and 6. The most likely reason for this could be that the section sliced for the 4000 cell spheroid is not done at the center. Hence, it is difficult to say with

certainty if a necrotic core is present in the 4000 cell spheroid or not. But there is a distinct difference in size when observing IF stained sample (figure 7 and 8) where liver specific markers are expressed at the center of the spheroid. This could contribute to the fact that no necrotic core is present in either size for at least 14 days.

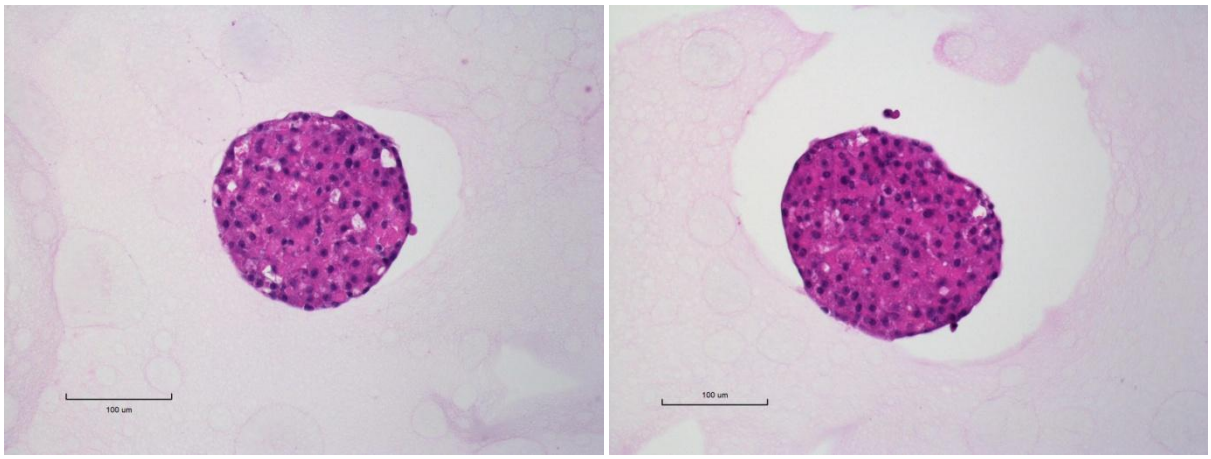

Figure 5. Hematoxyline and eosin staining of 2000 (left) and 4000 (right) cell spheroids at day 8.

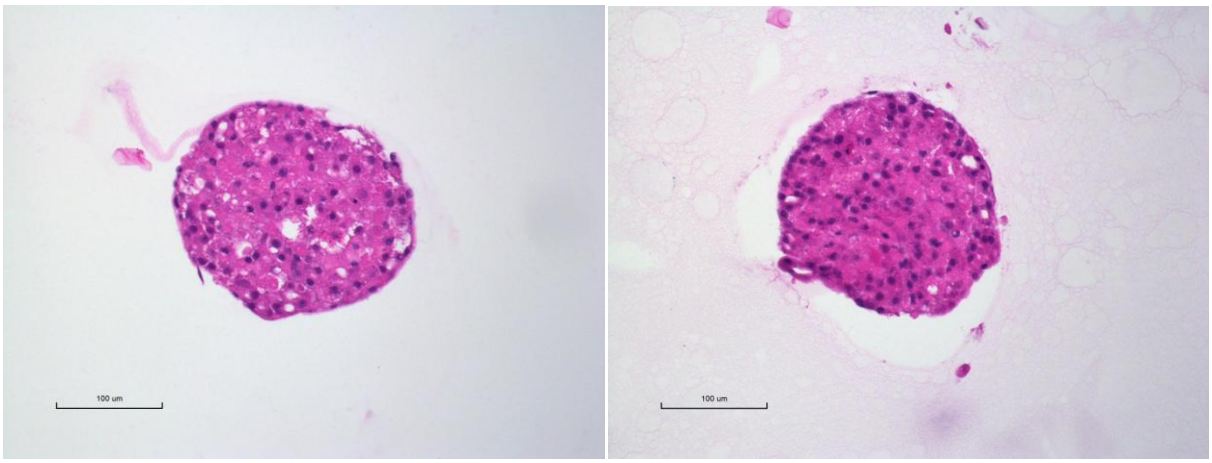

Figure 6. Hematoxyline and eosin staining of 2000 (left) and 4000 (right) cell spheroids at day 14.

The sections attained from Histocenter were also IF stained using primary and secondary antibodies. CK18, CK19, MRP2 and CYP3A4 primary antibodies were used for staining the samples. CK18 was used as a marker for detecting hepatocytes while CK19 was used for BECs. Figure 7, presented below, illustrates that CK18 and CK19 stained with the color green and red respectively are expressed at the centre of the spheroid. Fairly even polarization of both markers is also observed in both spheroid sizes. One remark on the 4000 cell spheroid is that there are more markers of CK18 expressed on the outer layer in comparison to CK19 which is mostly found at the center. This might indicate that the BECs tend to be situated inside the spheroid encapsulated by the hepatocytes on the outside.

A notable observation in figure 7 is that the 4000 cells spheroids seems to express more of CK18 while 2000 cell spheroid of CK19. The uneven expression of these markers could depend on a number of factors. One could be insufficient binding time of primary and/or secondary antibody which would result in less fluorescent color being emitted from cells when excited. The other factor could be inadequate binding due to low concentration of either of primary and/or secondary antibody. As this was an initial protocol for staining it

should be further optimized to find the optimal concentration for both primary and secondary antibody.

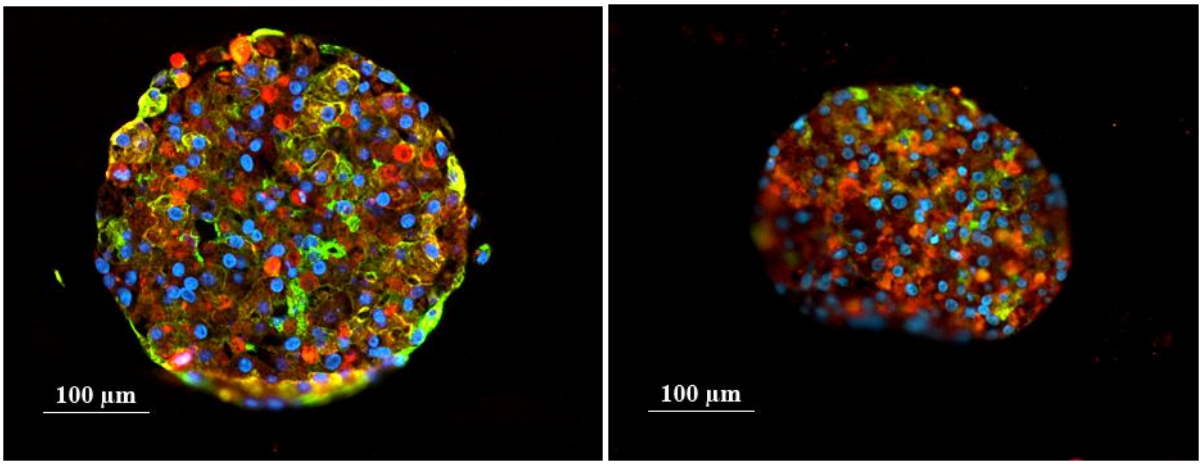

Figure 7. IF staining of a 2000 (right) and 4000 (left) cell spheroid section at day 8. The spheroids are stained with CK18 (Green) and CK19 (Red). The blue color represents hoechst which stains the nucleus.

The figure below (figure 8) illustrates the expression of MRP2 and CYP3A4 in green and red respectively. The staining of these markers was comparably more difficult than for CK18 and CK19. Unlike the staining of CK18 and 19 was somewhat was visibly associated to certain nuclei, MRP2 and CYP3A4 seem to create more of an artifact. This makes it difficult to confidently say which markers is expressed for which nucleus however the visual observation still indicates a mild expression of the markers.

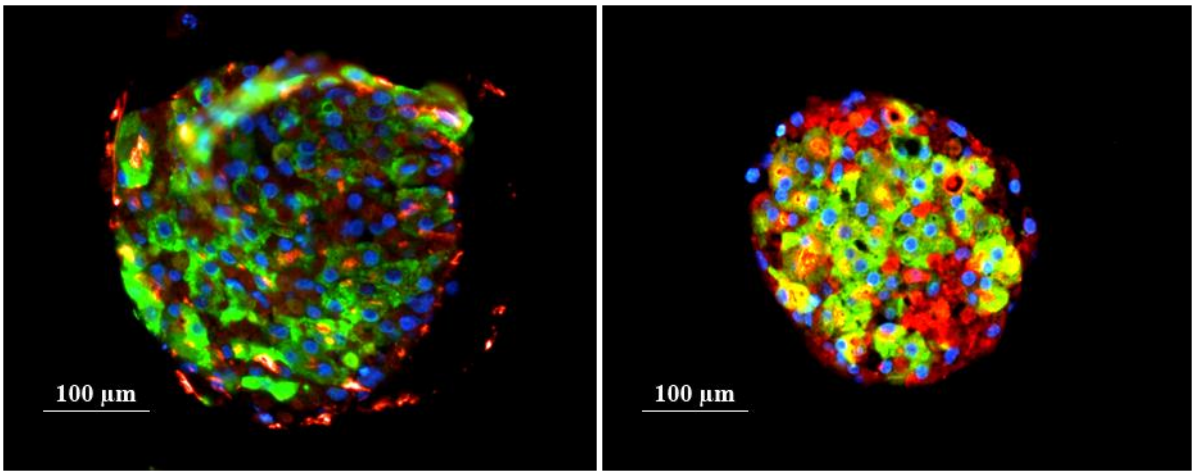

Figure 8. IF staining of a 2000 (right) and 4000 (left) cell spheroid section at day 8. The spheroids are stained with MRP2 (Green) and CYP3A4 (Red). The blue color represents hoechst which stains the nucleus.

With the HE staining of sectioned spheroids it was possible to observe that no or a very small necrotic core was formed in either spheroid size and for at least 14 days. IF staining further gave indication of liver specific markers being expressed, in various degrees, at the center of the spheroid. This gives recognition that chronic sustainability of both spheroid sizes is attainable.

4.3. Immunoflourescent Staining of Whole HepaRG Spheroids

Through the use of ImageXpress Micro XLS Widefield High-Content Analysis System it was possible to observe the presence and superficial polarization of liver specific markers. The built-in z-stack application was used to further enhance the spheroid markers and shape.

For the 2000 cell spheroids presented in figure 9 below, top row, it is observed that the hepatocyte marker CK18, and the BEC marker CK19 are both expressed. Additionally, both markers are expressed for at least 14 days. It is further noticed that the expression of CK18 is concentrated more towards the edges of the spheroids while CK19 is gathered inside. A similar trend is also observed in the larger spheroid size in figure 9. This observation supports indication found in the IF stained sections of spheroids where CK18 also seemed to focus more towards the edges and CK19 towards the center. In the human body BECs make up the biliary tract which often is situated in between hepatocyte cells. This natural spatial positioning might be the reason for how the cells arrange themselves in the spheroids. This however needs to be further investigated.

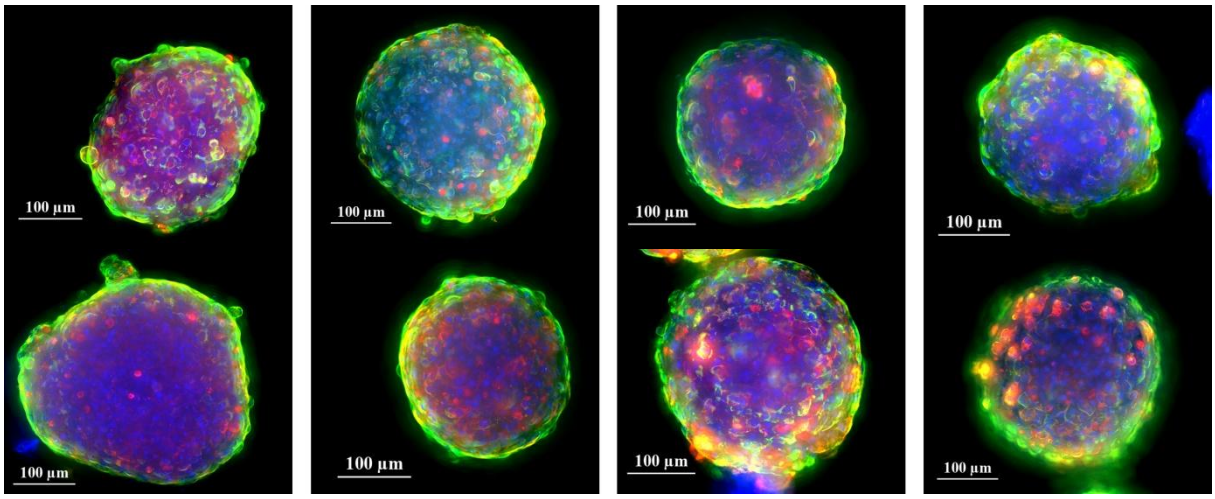

Figure 9. High content screening of CK18 (green) and CK19 (red) in whole spheroids with a size of 2000 cells (top row) and 4000 cells (bottom row) at different time points in the cultivation period. From left: day 3, 7, 10 and 14. The blue color represents hoechst which stains the nucleus.

While CK18 is observed to be concentrated towards the edge of the spheroids it might not be expressed as intensely. This is more likely the result of what could be called the 'halo effect'. The halo effect occurs especially when trying to capture a 3D object in 2D. Since several cells are stacked on each other towards the edges of the spheroid they will emit the fluorescent dye more intensely than single cells situated at the center of the spheroids. This gives the impression that cells towards the edge expresses more CK18 while in reality it is the combination of cells stacked on each other emitting fluorescent color at the same time.

The drug transporter marker MRP2 and phase I metabolic enzyme marker CYP3A4 are expressed in both spheroid sizes and for at least 14 days of the cultivation period as illustrated in figure 10. While MRP2 is illustrated more as an artifact of green in each spheroid the CYP3A4 is observed more closely to specific nucleuses. The expressions of these markers are further observed to be evenly distributed over the spheroid suggesting constant polarization in both spheroids sizes. The wider and more unspecific blue areas in

certain pictures (in both figure 9 and 10) are some form of contamination that has attached itself to the spheroid. To avoid this in the future, staining should be done in LAF benches.

It should be noted that each of these picture taken with the ImageXpress has been enhanced separately and can therefore not be compared with each other to give a relative understanding of how the expression level of each marker changes with time. This also explains why some spheroids express more of certain marker and less of the other. The staining protocol as mentioned previously when presenting the IF analysis results should also be taken into account. The protocol for staining of whole spheroids needs to be further optimized in 3 main prospects. The first is through optimizing the permeabilization of spheroid allowing antibodies to penetrate further towards the center. Second, increased binding time of both primary and secondary antibodies and third, an optimal dilution for each marker should be investigated.

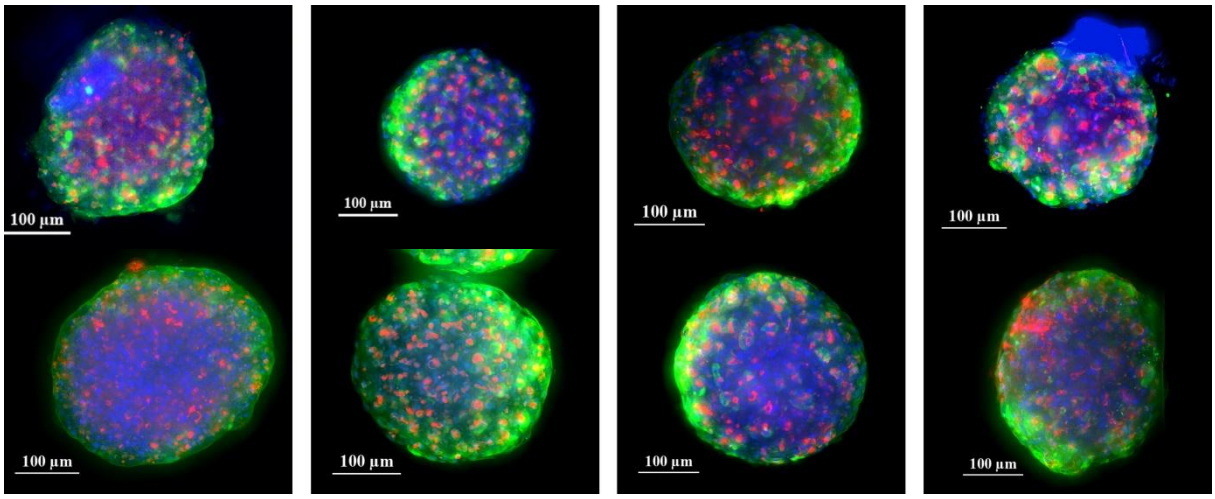

Figure 10. High content screening of MRP2 (green) and CYP3A4 (red) in whole spheroids with a size of 2000 cells at different time points in the cultivation period. From left: day 3, 7, 10 and 14. The blue color represents hoechst which stains the nucleus.

4.5. Gene expression of HepaRG spheroid culture

The gene expression of CYP1A2, CYP2C9, CYP3A4, MRP2, Ki67, CK19 and ALB were all measured in both spheroid sizes and for the whole cultivation period of 21 days. The results from these measurements are presented below in figure 11. It was found during the first run that extraction and isolation of RNA from the single spheroid sample at day 7 and by pooling 9 spheroids together was insufficient. When analyzing the purity of RNA using the Agilent 2100 Bioanalyser, no or insignificant concentration was detected. It was therefore decided that for the second run 30 spheroids will be pooled for gene expression analysis. Untreated HepaRG cells cultured in 2D and sampled at day 4 were used as a control to compare the results obtained from the second run. Furthermore, the results are compared between each spheroid size and for the whole cultivation period. Before presenting it should be noted that results from day 7 and 10 spheroid size 4000 are not presented due to loss of sample during the analysis.

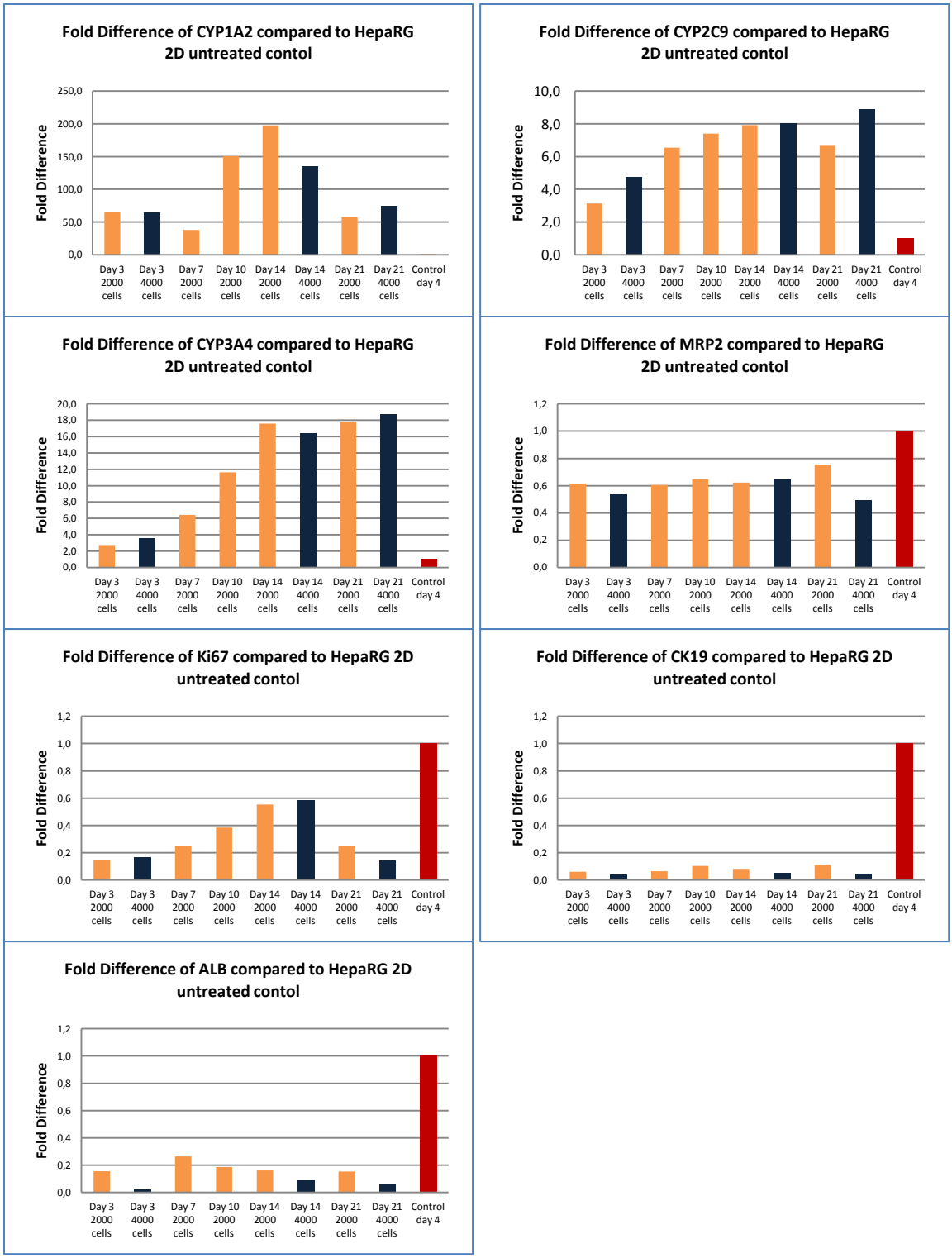

Figure 11. Gene expression of CYP1A2, CYP2C9, CYP3A4, MRP2, CK19, Ki67 and ALB during the 21 day cultivation period. The expression was compared with a control (HepaRG in 2D culture sampled at day 4).

The expression of each CYP enzyme proved to be higher than the HepaRG control during the whole cultivation period. For CYP1A2 it can be observed that the expression reaches a peak at day 14 where after it decreases during the following week. Whether this indicates a declining trend later on or retains stability needs to be further investigated. CYP2C9 expression on the other hand seems to increase until day 14 and remains relatively stable during the reaming cultivation period. The expression for CYP3A4 follows a similar trend

reaching a plateau expression after 14 days. This could imply that the spheroid conformation enhances and extends the CYP genes expression in comparison to 2D culture as a result of increase cell-cell interaction.

The drug transporter MRP2 kept a more or less constant expression level during the whole cultivation period and was comparably similar to the 2D control which might suggests that the 3D formation does not have an impact on the MRP2 protein. Ki67, the proliferation marker, was found to peak at day 14 where after the relative expression decreased. Since it represents proliferation of cells this could indicate an increase and/or decrease in size of the spheroids between day 7 and 21. However the size of spheroids remained the same throughout the cultivation period after day 3. This could possibly suggest that the gene, even though expressed, remains dormant or that minimum proliferation has occurred which is not visually observable. It was additionally observed that the expression level of Ki67 was less in 3D spheroids than in the 2D control. A previous study done using HepG2, which is a highly proliferative cell line when cultured in monolayer, showed a similar decrease in Ki67 expression when culture in spheroids [18]. This could indicate that culturing hepatocytes in spheroid structure inhibits proliferation of cells with time. The relative expression of both ALB and CK19 was found to be significantly lower in the spheroids than in the control. This observation is quite intriguing since ALB expression in hepatocytes has previously been shown to be higher when in spheroid structure in comparison to 2D [10, 18].

4.4. CYP1A2, CYP2D6, CYP2C9 and CYP3A4 enzyme activity

The CYP activity of each enzyme was followed over the course of 21 days and compared between the two different spheroid sizes by measuring the approximate concentration of each metabolite formed from their respective parent substance added. The result for each individual CYP enzyme activity is presented below in figure 13. It should be noted that no or insignificant concentration of the metabolite paracetamol (metabolized by CYP1A2) was found in all samples.

The pooled spheroids were firstly compared by observing their configuration before and after incubation to distinguish if possible aggregation occurred which might implicate the CYP activity. However, no aggregation of spheroids was found in either size during the 1h period during the experiment as illustrated in figure 12.

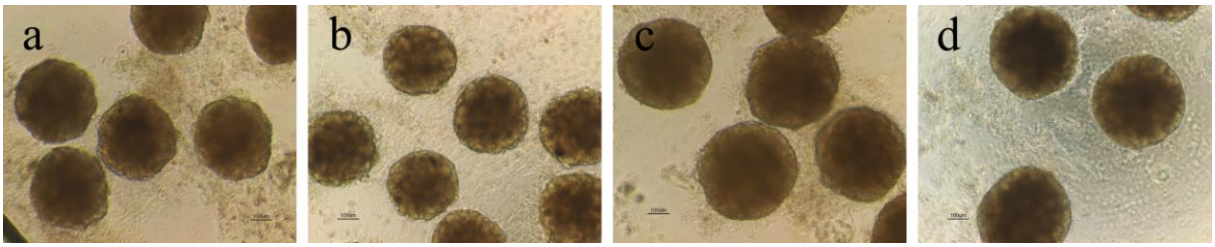

Figure 12. Spheroids pooled together, a and c, 2000 and 4000 cell spheroids before incubation, b and d, after incubation.

The concentration of each metabolite was observed to reach peak at day 7 were after it declined. The peak concentration of each metabolite in the 2000 cell spheroids was found to be 4.18, 27.37 and 2.51 pM/cell/h for 1'-OH-bufurlol, 4'-OH-diclofenc and 1'-OH-midazolam respectively. For the 4000 cell spheroids the peak was reached at 2.47, 14.12 and 1.39 pM/cell/h for 1'-OH-bufurlol, 4'-OH-diclofenc and 1'-OH-midazolam respectively. The

metabolite concentration of 1'-OH-bufuralol seems to remain stable from day 10 and onwards until the end of the cultivation period detecting slightly higher concentration at day 21 than day 14. 1'-OH-midazolam follows a similar trend as 1'-OH-bufuralol while the concentration of 4'-OH-diclofenac declines throughout the cultivation period as observed in figure 13. However the activity of CYP2C9 and CYP3A4 which metabolizes diclofenac and midazolam respectively does not follow a similar trend when observing the gene expression analysis. While the expression of these enzymes seems to increase toward day 14 and remain stable thereafter, the activity reaches a maximum at day 7 and declines towards the end of the cultivation period. A possible reason for this could be that the genes even though they are expressed for a longer time remain dormant. Another possible reason could be contamination of RNA samples which gives diverging results when compared to the activity.

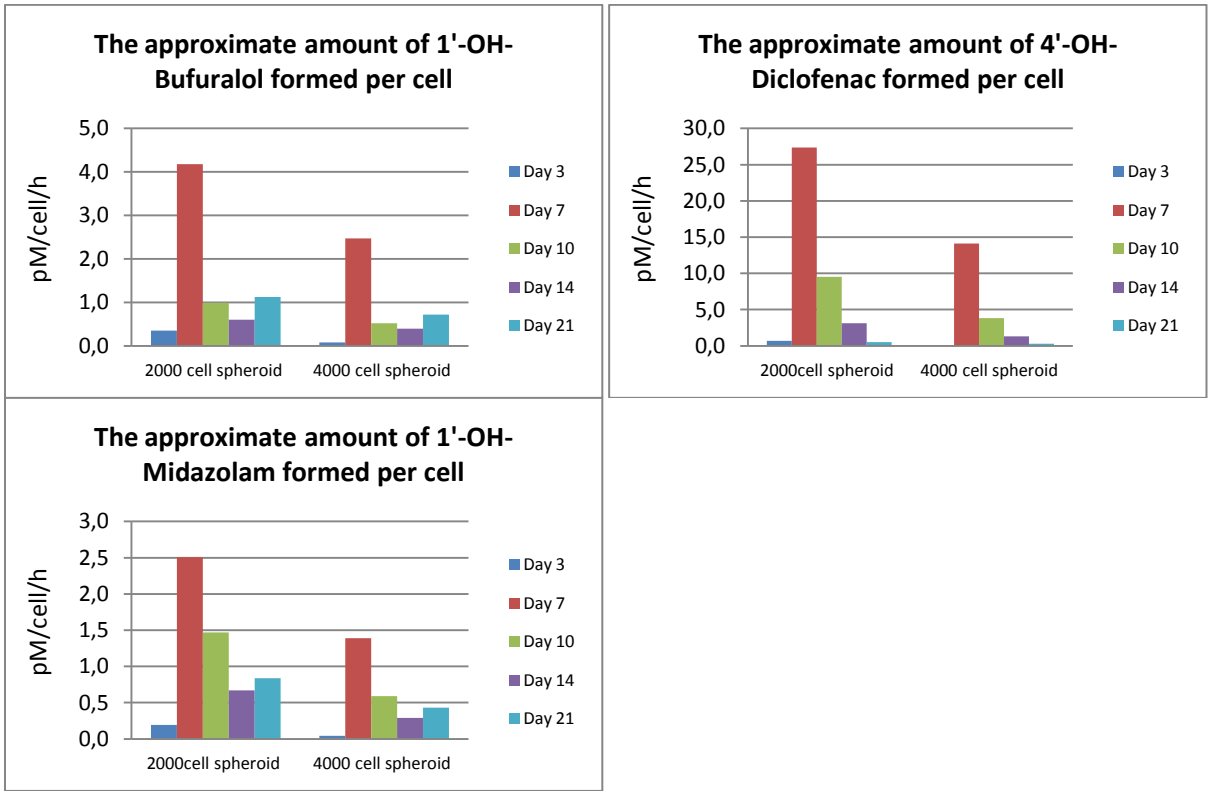

Figure 13. Enzyme activity of CYP2D6, CYP2C9 and CYP3A4 measuring the amount of 1'-OH-Bufuralol, 4'-OH-Diclofenac and 1'-OH-Midazolam respectively formed per cell.

For the activity analysis at day 3, spheroids had not been introduced to HepaRG culture medium containing approximately 2% DMSO which is known to up-regulate the CYP activity. Hence, the concentrations of metabolites found at day 3 are considerably lower than for the other samples days.

Initial observation of figure 13 shows that the smaller size has a higher enzymatic activity. Although, it should be taken in to account that the calculations presumes full activity of every cell in the spheroid. However it is known that the formation of a spheroid model tends to create a diffusion gradient which could possible explain the difference in activity between the two sizes. Substances' depending on various factors diffuses at different speed. Additionally a larger size of the spheroid increases the distance of substance diffusion to the center. Parent substances might therefore not have been able to fully diffuse during the 1h incubation into the center of the 4000 cell spheroid leaving a large part of it inactive.

Previous studies have stated that the expression and activity of CYP2D6 is weaker in the HepaRG cell line when cultured in monolayer [8, 27, 28, 44]. It is further speculated that it is donor dependent meaning that the cell line is isolated from a patient with poor expression of that gene [28]. This thesis has on the other hand shown that the activity of CYP2D6 when cultured in spheroid formation is not only detected but is kept for as long as 21 days with a peak activity at day 7. CYP1A2 which metabolizes phenacetin showed no activity during the whole cultivation period. The gene expression level however increased up until day 14 where after it declined throughout the cultivation period. This was found to be peculiar since it has previously been stated that CYP1A2 has been found to express and function at a similar level in HepaRG as in PHH and that it is comparatively higher than CYP2D6 [8]. This might be an initial indication that culturing HepaRG cells in spheroid formation in the case of CYP2D6 enhances the expression while simultaneously improving and sustaining the activity whereas the opposite is true for CYP1A2. To verify this, gene expression analysis of CYP2D6 and further activity analysis on CYP1A2 should be investigated.

5. Conclusion

This thesis has focused on developing and characterizing a 3D *in vitro* spheroid model for the purpose of drug uptake, metabolism and transport studies using HepaRG cell line and ultra-low attachment plates. The HepaRG cells aggregated and formed a spheroid structure approximately 3 days after they had been plated independent of the cellular concentration. During the first run it was evidently decided that the 500 cell spheroid was not applicable for various analysis due to its small and inconvenient size. The absence of a necrotic core combined with the presence and even polarization of liver specific markers (CK18, CK19, MRP2 and CYP3A4) confirmed that chronic sustainability of both 2000 and 4000 cell spheroid is attainable. Gene expression analysis reveled that the drug transporter marker MRP2 was expressed evenly during the whole cultivation period and at a level similar to 2D HepaRG control. The marker Ki67 although varying in expression showed no indication of proliferation as no significant change in size was detected during the run. Hepatocyte and BEC genes ALB and CK19 respectively had significantly low relative expression in spheroid formation compared to 2D culture however the reason for this is still unknown. The gene expression analysis also indicated that the spheroid model enhances and extends the expression of CYP genes, CYP1A2, CYP2C9 and CYP3A4 in comparison to 2D culture. However the activity for CYP2D6, CYP2C9 and CYP3A4 all reached a maximum at day 7 where after it declines towards the end of the cultivation period while CYP1A2 showed no sign of activity during this time.

In summary an initial 3D *in vitro* spheroid model using HepaRG cell line has been developed which is able to maintain cellular viability, express various liver specific markers and enables long-term liver functionality however further experimentations and investigation needs to be conducted in order confirm and optimize the model for its purpose.

6. Future Studies

Future studies on the liver spheroid model will need to include additional examination on CYP activity allowing more accurate and reliable results to be obtained. This should include observing the activity around day 7 to understand the peak activities attained in this thesis. Furthermore, the metabolite formation should be related to mg protein which would allow spheroid samples to be more accurately compared. Supplementary gene expression analysis of CYP enzymes should also be included to complement the activity. Analysis on ALB and CK19 gene expression needs to be conducted in order to verify the results found in this thesis. If similar results are found, further experiments needs to be conducted to better understand the reason for the low expression levels. Protocol for staining sections and whole spheroids using primary and secondary antibodies has to be further optimized. A possible procedure is to do a dilution series from which an appropriate concentration for both staining techniques can be found.

It would be interesting to investigate the effect of DMSO on the spheroid activity. This can be done by parallel culturing of spheroids in both HepaRG culture medium (containing ~2% DMSO) and HepaRG induction medium (no DMSO). CYP activity of spheroids cultured in the two different medium should be measured and complemented with protein measurement.

Bibliography

1. Tso, P. and J. McGill, *The Physiology of the Liver*. 2003, A. George, Tanner and A. Rodney Rhoades Medical Physiology, Second edition, Lippincott, Williams & Wilkins:(in press).
2. Verhulsel, M., et al., *A review of microfabrication and hydrogel engineering for micro-organs on chips.* Biomaterials, 2014. **35**(6): p. 1816-1832.
3. Borlak, J., A. Chougule, and P.K. Singh, *How useful are clinical liver function tests in vitro human hepatotoxicity assays?* Toxicology in Vitro, 2014. **28**(5): p. 784-795.
4. Ahuja, V. and S. Sharma, *Drug safety testing paradigm, current progress and future challenges: an overview.* Journal of Applied Toxicology, 2014. **34**(6): p. 576-594.
5. Sasseville, V., et al., *Testing paradigm for prediction of development-limiting barriers and human drug toxicity.* Chemico-biological interactions, 2004. **150**(1): p. 9-25.
6. Huh, D., G.A. Hamilton, and D.E. Ingber, *From 3D cell culture to organs-on-chips.* Trends in Cell Biology, 2011. **21**(12): p. 745-754.
7. Braeuning, A., et al., *Recent advances in 2D and 3D in vitro systems using primary hepatocytes, alternative hepatocyte sources and non-parenchymal liver cells and their use in investigating mechanisms of hepatotoxicity, cell signaling and ADME.* 2013.
8. Marion, M.-J., O. Hantz, and D. Durantel, *The HepaRG cell line: biological properties and relevance as a tool for cell biology, drug metabolism, and virology studies*, in *Hepatocytes*. 2010, Springer. p. 261-272.
9. Gunness, P., et al., *3D organotypic cultures of human HepaRG cells: a tool for in vitro toxicity studies.* Toxicological sciences, 2013. **133**(1): p. 67-78.
10. Wang, Z., et al., *HepaRG culture in tethered spheroids as an in vitro three-dimensional model for drug safety screening.* Journal of Applied Toxicology, 2014.
11. DeLeve, L.D., *Vascular liver disease and the liver sinusoidal endothelial cell*, in *Vascular Liver Disease*. 2011, Springer. p. 25-40.
12. Monga, S.P. and P.T. Cagle, *Molecular pathology of liver diseases*. Vol. 5. 2010: Springer Science & Business Media.
13. Hughes, B., *Industry concern over EU hepatotoxicity guidance.* Nat Rev Drug Discov, 2008. **7**(9): p. 719-719.
14. Ou, K.-L. and H. Hosseinkhani, *Development of 3D in vitro technology for medical applications.* International journal of molecular sciences, 2014. **15**(10): p. 17938-17962.
15. Damania, A., E. Jain, and A. Kumar, *Advancements in in vitro hepatic models: application for drug screening and therapeutics.* Hepatology International, 2014. **8**(1): p. 23-38.
16. Vellonen, K.-S., et al., *A critical assessment of in vitro tissue models for ADME and drug delivery.* Journal of Controlled Release, 2014. **190**: p. 94-114.
17. Khoruzhenko, A., *2D-and 3D-cell culture.* Biopolymers and Cell, 2011(27): p. 17-24.
18. Ramaiahgari, S.C., et al., *A 3D in vitro model of differentiated HepG2 cell spheroids with improved liver-like properties for repeated dose high-throughput toxicity studies.* Archives of toxicology, 2014. **88**(5): p. 1083-1095.
19. Kleinman, H.K., D. Philp, and M.P. Hoffman, *Role of the extracellular matrix in morphogenesis.* Current opinion in biotechnology, 2003. **14**(5): p. 526-532.

20. Baptista, P.M., et al., *The use of whole organ decellularization for the generation of a vascularized liver organoid.* Hepatology, 2011. **53**(2): p. 604-617.
21. Pampaloni, F., E.G. Reynaud, and E.H.K. Stelzer, *The third dimension bridges the gap between cell culture and live tissue.* Nat Rev Mol Cell Biol, 2007. **8**(10): p. 839-845.
22. Sabetkish, S., et al., *Whole-organ tissue engineering: Decellularization and recellularization of three-dimensional matrix liver scaffolds.* Journal of Biomedical Materials Research Part A, 2014.
23. Crapo, P.M., T.W. Gilbert, and S.F. Badylak, *An overview of tissue and whole organ decellularization processes.* Biomaterials, 2011. **32**(12): p. 3233-3243.
24. Murphy, S.V. and A. Atala, *3D bioprinting of tissues and organs.* Nature biotechnology, 2014. **32**(8): p. 773-785.
25. Landry, J., et al., *Spheroidal aggregate culture of rat liver cells: histotypic reorganization, biomatrix deposition, and maintenance of functional activities.* The Journal of cell biology, 1985. **101**(3): p. 914-923.
26. Astashkina, A. and D.W. Grainger, *Critical analysis of 3-D organoid in vitro cell culture models for high-throughput drug candidate toxicity assessments.* Advanced drug delivery reviews, 2014. **69**: p. 1-18.
27. Kanebratt, K.P. and T.B. Andersson, *Evaluation of HepaRG cells as an in vitro model for human drug metabolism studies.* Drug metabolism and disposition, 2008. **36**(7): p. 1444-1452.
28. Guillouzo, A., et al., *The human hepatoma HepaRG cells: a highly differentiated model for studies of liver metabolism and toxicity of xenobiotics.* Chemico-biological interactions, 2007. **168**(1): p. 66-73.
29. Chatterjee, S., *Cytokeratins in health and disease.* Oral and maxillofacial pathology journal, 2012. **3**(1): p. 198-202.
30. Schweizer, J., et al., *New consensus nomenclature for mammalian keratins.* The Journal of cell biology, 2006. **174**(2): p. 169-174.
31. Thapa, B. and A. Walia, *Liver function tests and their interpretation.* The Indian Journal of Pediatrics, 2007. **74**(7): p. 663-671.
32. Sharma, O.P., *Clinical Biochemistry of Hepatotoxicity.* Journal of Clinical Toxicology.
33. Deeley, R.G. and S.P. Cole, *Multidrug resistance protein*. 1996, Google Patents.
34. Sekine, T., H. Miyazaki, and H. Endou, *Molecular physiology of renal organic anion transporters.* American Journal of Physiology-Renal Physiology, 2006. **290**(2): p. F251-F261.
35. Borst, P., et al., *A family of drug transporters: the multidrug resistance-associated proteins.* Journal of the National Cancer Institute, 2000. **92**(16): p. 1295-1302.
36. Bakos, É., et al., *Interactions of the human multidrug resistance proteins MRP1 and MRP2 with organic anions.* Molecular Pharmacology, 2000. **57**(4): p. 760-768.
37. Scholzen, T. and J. Gerdes, *The Ki67 protein: from the known and the unknown.* Journal of cellular physiology, 2000. **182**(3): p. 311-322.
38. Gonzalez, F.J. and R.H. Tukey, *Drug metabolism.* Goodman & Gilman's The Pharmacological Basis of Therapeutics. 11th ed. New York, NY: McGraw-Hill, 2006: p. 71-91.
39. Testa, B. and S. Krämer, *The Biochemistry of Drug Metabolism: Volume 1: Principles, Redox Reactions, Hydrolyses.* Zurich and Weinheim: VHCA and Wiley-VCH, 2008.

40. Zanger, U.M. and M. Schwab, *Cytochrome P450 enzymes in drug metabolism: regulation of gene expression, enzyme activities, and impact of genetic variation.* Pharmacology & therapeutics, 2013. **138**(1): p. 103-141.
41. Seng, K.C., et al., *Frequency of cytochrome P450 2C9 (CYP2C9) alleles in three ethnic groups in Malaysia.* Asia-Pacific Journal of Molecular Biology and Biotechnology, 2003. **11**(2): p. 83-91.
42. Abraham, B.K. and C. Adithan, *Genetic polymorphism of CYP2D6.* Indian Journal of Pharmacology, 2001. **33**(3): p. 147-169.
43. McIntyre, A., et al., *Carbonic anhydrase IX promotes tumor growth and necrosis in vivo and inhibition enhances anti-VEGF therapy.* Clinical Cancer Research, 2012. **18**(11): p. 3100-3111.
44. Aninat, C., et al., *Expression of cytochromes P450, conjugating enzymes and nuclear receptors in human hepatoma HepaRG cells.* Drug Metabolism and Disposition, 2006. **34**(1): p. 75-83.